

# Methodology of wheat lodging annotation based on semi-automatic image segmentation algorithm

Gan Zhang<sup>1</sup>, Fangming He<sup>1</sup>, Haifeng Yan<sup>1</sup>, Haifeng Xu<sup>1,2</sup>, Zhenggao Pan<sup>1,2</sup>,  
Xiaoying Yang<sup>1,2</sup>, Dongyan Zhang<sup>1</sup>, Weifeng Li<sup>1\*</sup>

(1. National Engineering Research Center for Agro-Ecological Big Data Analysis and Application, Anhui University, Hefei 230601, China;  
2. College of Engineering, Suzhou University, Suzhou 234000, China)

**Abstract:** The existing identification of wheat lodging based on unmanned aerial vehicle (UAV) is significantly dependent on the artificial ground annotation method, which exhibits low annotation accuracy and strong subjectivity, thus resulting in a low degree of separation for the annotated lodging area and the non-lodging area. To solve the problem of insufficient applicability of traditional annotation research to agricultural images, especially wheat field lodging images, a lodging annotation method in the study based on semi-automatic image segmentation algorithm was proposed. Firstly, a total of 101 farmlands with lodging occurred during the flowering, filling and mature period of wheat in 2019 and 2021 were segmented as the research objects. The above images were respectively changed into RGB and HSV color space and converted into four vegetation indexes, including excess-green (ExG), green leaf index (VEG), normalized green-red difference index (NGRDI), as well as red-green ratio index (GRRI). Secondly, lodging regions were extracted and modified from the image in accordance with color features. Lastly, the JM distance of lodging and non-lodging areas served as an index to examine the effect of image annotation for data analysis and evaluation of segmentation accuracy. The result of the experiment indicated that there was a very significant difference between the JM distance based on the annotation method proposed in this study and the result based on manual annotation. GRRI and ExG were the most suitable features for image annotation. The method proposed in this study had high generalization performance for the images captured in the three fertility periods in 2019 and 2021, and the images with poor image annotation results took up a small proportion. In brief, the lodging area annotation method proposed in this study increases the annotation accuracy by extracting lodging areas using a semi-automatic image segmentation algorithm. The proposed method outperforms the manual annotation method.

**Keywords:** semi-automatic image annotation, wheat lodging, unmanned aerial vehicle, image processing, feature separability

**DOI:** 10.33440/ijpaa.20220501.193

**Citation:** Zhang G, He F M, Yan H F, Xu H F, Pan Z G, Yang X Y, Zhang D Y, Li W F. Methodology of wheat lodging annotation based on semi-automatic image segmentation algorithm. *Int J Precis Agric Aviat*, 2022; 5(1): 47–53.

## 1 Introduction

Wheat as one of the critical food crops in the world, it is extensively grown in northern China. Lodging always reduces the yield of grain crops (e.g., wheat) heavily from 7% to 35%<sup>[1]</sup>. Relevant studies have shown that wheat lodging may affect agricultural mechanization operations, reduces the quality of grains, and more even, induce diseases<sup>[2]</sup>. Accordingly, non-destructive and instant monitoring wheat lodging is important to the yield increasing, disaster preventing, and property insuring.

Monitoring crops lodging is required to photograph the lodging area in time. However, taking these pictures is a time- and energy-constrained task, since the work usually is conducted using the field survey method, which also decreases the accuracy and

efficiency of photographing. As remote sensing techniques have been leaping forward, a novel method, UAV-based image processing technology, has progressively replaced the field survey method as the main technology for crops lodging monitoring<sup>[2]</sup>.

Recent researches have suggested that using UAV-based image processing technology will increase the accuracy and efficiency of monitoring crops lodging significantly. For instance, Dong et al. employed the minimum distance method, maximum likelihood method, neural network, and support vector machine to extract the lodging area of winter wheat, the maximum likelihood method has the optimal classification accuracy of 95.15%<sup>[3]</sup>. Yang et al. used machine learning to make decisions tree classification, adding single feature probability (SFP) feature screening technology. It can identify wheat lodging areas with an accuracy rate of 96.17%<sup>[4]</sup>. Tian et al. used the partial least squares discriminant method to build a rice normal/lodging classification model in accordance with the full-band spectral reflectance, and the accuracy of the normal rice and lodging rice identification reaches 98.10% and 99.04% respectively<sup>[5]</sup>. Li et al. used the K-Means algorithm to extract winter wheat, and the accuracy could reach 86.44%<sup>[6]</sup>. Ren et al. used object-oriented multi-scale segmentation and random forest methods to segment and classify UAV aerial photography data, and extracted the lodging area of crops. The classification error ranged from 0.46% to 1.11%<sup>[7]</sup>.

Lodging area segmentation is the core of monitoring wheat lodging by UAV-based image processing techniques. Moreover,

**Received date:** 2022-10-18 **Accepted date:** 2022-12-24

**Biographies:** **Gan Zhang**, PhD, research interests: precision agriculture aviation technology and equipment, Email: 1092889508@qq.com. **Fangmin He**, Postgraduate student, research interests: agricultural remote sensing, Email: 1473375700@qq.com. **Haifeng Yan**, Postgraduate student, research interests: image processing and analysis, Email: 1135678731@qq.com. **Haifeng Xu**, PhD, research interests: data mining, Email: xuhaifeng@ahszu.edu.cn. **Zhenggao Pan**, PhD, research interests: artificial intelligence, Email: szxypzg@163.com. **Xiaoying Yang**, Master degree, research interests: agricultural IoT, Email: yangxiaoying@ahszu.edu.cn. **Dongyan Zhang**, PhD, research interests: precision agriculture aviation, Email: zhangdy@ahu.edu.cn.

\***Corresponding author:** **Weifeng Li**, Engineer, research interests: agricultural aviation application. Email: 597622251@qq.com.

lodging area annotation is an essential step in lodging area segmentation. However, unlike the other image segmentation tasks, it is difficult to depict the boundaries between lodging and non-lodging areas when labling wheat lodging area using UAV images. The reason is that some lodging and non-lodging areas are relatively close in color and texture features. The objectivity and accuracy of manual labling are low, and it is difficult to meet the requirements of image segmentation algorithm development<sup>[8-11]</sup>. There is huge labling workload of large-scale remote sensing images, and efficient image labling technology is urgently required to reduce the resource consumption of dataset production. Image annotation methods can be classified as model-based, learning-based, label length-based, dataset-based methods<sup>[12]</sup>. The model-based image annotation method are primarily introduced based on the characteristics of crop lodging area identification task, in this study, which is one of the most extensively used image annotation methods. The annotator lables the region of interest according to the characteristics of the images. The method can be classified as generative models<sup>[13-15]</sup>, discriminative models<sup>[16-19]</sup>, graph-based models<sup>[20-22]</sup> and nearest neighbor-based models<sup>[23-25]</sup>. For instance, Ke et al. proposed a hierarchical image annotation model, which used a two-layer structure of discriminative and generative layers to achieve automatic annotation of extended related image sets [15]. Yu et al. proposed a new multi-directional search framework for semi-automatic annotation propagation. Manually annotated images input by the user were employed for clustering when interacting with the annotation system. The annotation guidance algorithm was generated, and the accuracy was obtained in the continuous image input process to guide the user to make more accurate annotation<sup>[19]</sup>. To solve the problem that the semantic gap between low-level visual features and high-level semantic concepts affect the quality of image annotation, Wang et al. proposed a hierarchical-double loop algorithm to improve the quality of annotations, and proposed another centroid-based convergence method to automatically assign relevant multiple keywords to user-specified images, which can significantly increase retrieval accuracy and fast response requirements<sup>[26]</sup>.

At present, most researches on image annotation are layered image annotation methods for specific scenes, and most verification images are public datasets<sup>[27-29]</sup>. Related researches on agricultural images, especially wheat field images, is relatively lacking, which leads to the lack of effective tools for wheat field image annotation. In this study, an annotation method for wheat field lodging based on semi-automatic image segmentation algorithm was proposed. The characteristics of the wheat field lodging annotation task were analyzed. Targeted solutions were proposed based on previous studies and the method was verified by using the data set of lodging images of wheat fields in the whole phenological period.

## 2 Materials and Methods / Related Works

### 2.1 Experimental materials

The experimental site was located in Baihu farm, Lujiang County, Hefei City, Anhui Province, China (31°13'25.7"N, 117°27'48.8"E), i.e., a main wheat growing area in China with a mild climate and an average annual precipitation of nearly 1000 mm. The common natural disasters in this region are rainstorms, floods and typhoon. Wheat lodging is prone to occur.

The wheat sown in the experimental field were 10 varieties commonly planted in the Jianghuai region of Anhui (Table 1).

**Table 1. Experimental wheat variety**

Yang mai 13	Ning mai 13
Yang mai 19	Yang mai 22
Yang mai 9	Ning mai 9
Wanxi mai 0638	Shen xuan 6
Yang mai 15	Yang mai 24

### 2.2 Image acquisition

The DJI Phantom 4 Pro quadrotor UAV was adopted to collect low-altitude remote sensing images. The DJI Phantom 4 Pro camera is a 20-megapixel high-definition digital camera. The maximum effective distance for image acquisition is 2 km, and the battery life is 30 minutes. The performance parameters of the sensor are listed in Table 2.

**Table 2 Parameters of DJI phantom 4 pro HD digital camera**

Parameters	Values
Type	CMOS
Effective pixels	20 million
Field of view (FOV)	84°
Image size	5472×3648
Image format	JPG
ISO range	100 to3200
Shutter speed	8s to1/8000 s
Focal length	8.8 mm
Number of channels	3(R, G, B)

GSP (Ground Station Pro, DJI CO., China) software was adopted to plan the route for image acquisition. In this study, the UAV flight height was set to 40 m, the image heading overlap was 80%, and the image lateral overlap was 80%. During the image acquisition process, in order to reduce the influence of weather conditions on image acquisition, the image acquisition time was between 11:00-12:00, and the weather was sunny and windless.

The image acquisition data were range from April to May in 2019 and 2021. The images of the lodging wheat fields were taken during the three phenological periods of wheat (flowering period, filling period and mature period). Figure 1 presents the collected wheat field images. The phenological period and weather conditions of the experimental area are listed in Table 3.

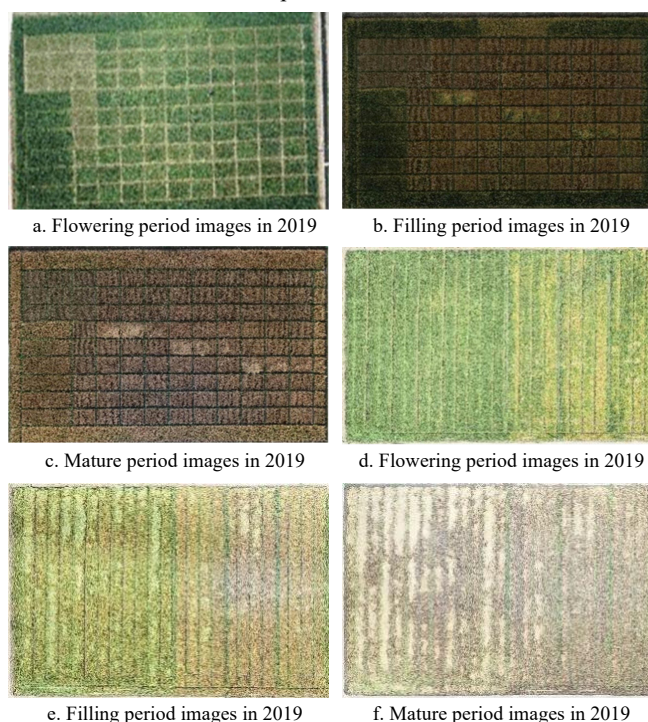


Figure 1 Examples of visible light RGB images

**Table 3** Details of experimental data

Year	Date	Weather	Phenological period	Number of lodging fields
2019	April 17	sunny	flowering period	14
	May 9	sunny	filling period	14
	May 18	sunny	mature period	20
2021	May 1	sunny	flowering period	12
	May 8	sunny	filling period	20
	May 18	sunny	mature period	21

In this study, a total of six UAV imagetasks were carried out. After each flight, the original images were stitched to obtain the UAV images of the entire wheat field experimental plot, with a ratio of nearly 7600×5800.

### 2.3 Research method

In this study, Halcon12 was employed to compile image processing algorithms, python was adopted to write distance calculation algorithms, image stitching was implemented by DJI Pix4Dmapper software, and Labelme software was used for conventional image annotation.

#### 2.3.1 Lodging area annotating method

The conventional lodging image annotation mostly adopts the model-based image annotation method. Based on the color, texture and other characteristics of remote sensing images in different features, researchers visually distinguish lodging and non-lodging areas, and use image annotation tools (e.g., Labelme) to annotate lodging areas in the image. The boundary of the lodging area annotated using the above method relies on the subjective visual perception of the annotator. The accuracy and consistency of the annotating cannot meet the requirement, which may result in a small difference in the gray value of the image between the lodging area and the non-lodging area. It is difficult to increase the accuracy of subsequent segmentation algorithms.

To solve the problems above, a method for annotating wheat field lodging based on semi-automatic image segmentation algorithm was proposed. The steps of the method were as follows (Figure 2): (1) The edge detection algorithm was employed to identify the edge of the field and the stitched images were transformed into multiple sub-images based on the field edge. (2) Sub-image was converted into the optimal feature. (3) Image segmentation algorithm was adopted to segment lodging area from the image to obtain a roughly segmented image. The image segmentation algorithm could apply a fixed threshold, an automatic threshold or a region growing method. (4) In accordance with the image text information, edge of the lodging area was manually corrected to obtain more accurate segmented images.

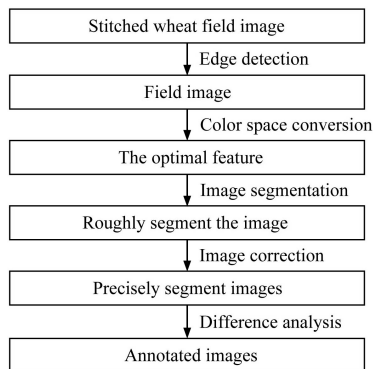


Figure 2 Lodging area annotation process

The key for the lodging area annotation refers to the optimal feature selection. The optimal feature would be selected by comparing the accuracy of annotated images in different features.

The annotated results with significant difference between lodging areas and non-lodging areas is easy to accurately segmented. It indicates that the lodging areas and non-lodging areas are accurately annotated.

Lastly, this method was verified for effectiveness (Whether it achieves better results than manual annotation) and generalization performance (Whether the method can be applied to images of different reproductive periods in different years) by experiments.

#### 2.3.2 Method for measuring the accuracy of annotation

In remote sensing, JM distance is usually used to examine the difference between two types of ground objects<sup>[30,31]</sup> (Formula (1)-(3)).

$$JM(\omega_i, \omega_j) = \int_x \left( \sqrt{p(x|\omega_i)} - \sqrt{p(x|\omega_j)} \right)^2 dx \quad (1)$$

where,  $\omega_i$  and  $\omega_j$  represents two different types of ground cover;  $p(x|\omega_i)$  and  $p(x|\omega_j)$  are the conditional probability density, i.e., the probability of the  $i$ th and  $j$ th pixels belong to the  $\omega_i$  or  $\omega_j$  class.

$$JM = 2(1 - e^{-B}) \quad (2)$$

$$B = \frac{1}{8}(\mu_j - \mu_k)^T \left( \frac{\sum j + \sum k}{2} \right)^{-1} (\mu_j - \mu_k) + \frac{1}{2} \ln \left( \frac{\left| \frac{\sum j + \sum k}{2} \right|}{\sqrt{|\sum j| |\sum k|}} \right) \quad (3)$$

where,  $u_i$  and  $u_j$  denote the average spectral reflectance of a specific type;  $\Sigma_i$  and  $\Sigma_j$  express the unbiased estimate of the  $i$  and  $k$  covariance matrices for a specific type.

The value of JM distance ranges from 0 to 2. A large J-M distance indicates that the difference between the two types of ground objects is more significant, thus contributing to the separation of the two types<sup>[32]</sup>. Table 4 lists the classification of JM distance feature separability.

**Table 4** Separability classification of JM distance features

JM distance interval	Grading
JM<0.5	Very poor
JM≥0.5 or JM<1.25	Poor
JM≥1.25 or JM<1.75	Generally good
JM≥1.75	Good

In this study, JM distance was employed as index for feature selection. The images were converted into different features and annotated using the method presented in 2.3.1 section. The JM distance between the lodging and non-lodging area of the annotated was calculated. The feature with the maximum JM distance was the optimal feature.

#### 2.3.3 Research Process

In this study, experiments were designed for to select features and verify the effectiveness of the image annotation method. The experiments were divided into three steps: field division, image annotation and JM distance analysis.

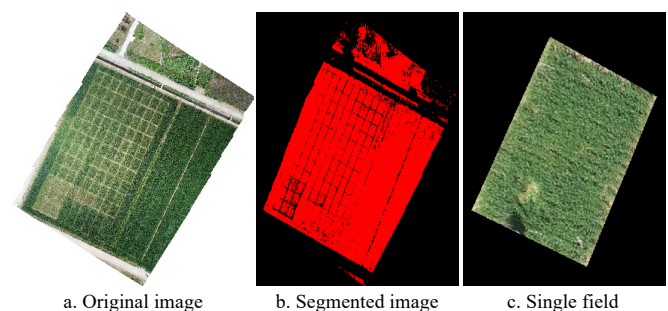


Figure 3 Field division



First, fields diving. Six stitched low-altitude remote sensing images of wheat fields collected in 2019 and 2021 were selected as the analysis objects, and the fields were divided by identifying road. The images were divided into 101 small fields (plots) (Figure 3).

Secondly, lodging area annotation. According to the method in Section 2.2, the 101 wheat field images containing lodging were converted into different features. 10 feature were selected as the candidate features, including RGB (including R, G, B, 3 channels), HSV (including H, S, V, 3 channels), ExG (Eq. (4)), VEG (Eq. (5)), NGRDI (Eq. (6)) and GRRRI (Eq. (7)). Then, threshold segmentation method was selected to segment the lodging area and blob analysis method was employed to remove the tiny connected domains, fill the voids, and optimize the extraction results of the lodging areas. Lastly, the lodging region extraction result was manually reviewed. The lodging segmentation result was modified as the final result of the lodging region annotation according to the semantic information around the image pixels.

$$2G - R - B \quad (4)$$

$$G / R^a B^{(1-a)}, a = 0.667 \quad (5)$$

$$(G - R) / (G + R) \quad (6)$$

$$G / R \quad (7)$$

where, R, G, B represent the R, G, B channels of the RGB color space respectively.

RGB and HSV are tradition universal features, the combination of RGB and HSV can completely reflect all features of the image. ExG, VEG, NGRDI, GRRRI are special image features. These features had been widely used in the field of remote sensing image processing. The current research has not determined the optimal feature extraction for lodging area segmentation. Therefore, the above channels and vegetation index are used as candidate features in this paper.

Finally, algorithm validity verification, feature selection and algorithm generalization performance test were performed.

To verify the effectiveness of the method proposed, the JM distance of all the annotated images (one image was converted into 10 features) for lodging and non\_lodging areas was obtained. It was compared with the JM distance of manual annotated images.

To select the optimal feature, JM distance of the algorithm annotated images was compared, and the feature with the maximum JM distance would be selected.

To validate the generalization performance, the JM distances of the wheat field image annotation results of different phenological periods in 2019 and 2021 were compared, and the consistency of the JM distance becomes an indicator to examine the generalization performance of the algorithm.

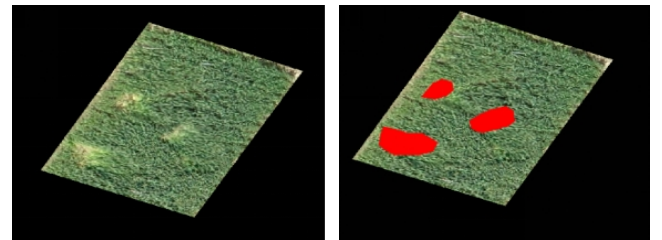
**Table 5 Data Analysis Experiments and Objectives**

Experiment type	Experiment target
(1) Comparison experiment of algorithm annotation and manual annotation results	Verify that the image annotation algorithm proposed in this study is better than manual annotation
(2) Comparison experiment of algorithm annotating results in different features	Get the optimal feature for image annotation
(3) Comparison experiment of algorithm annotating results under different phenological period	Test the generalization of the algorithm to remote sensing images of wheat fields in different fertility periods

### 3 Results and Discussion

The UAV-images were annotated using the method proposed in this study, and the result is presented in this section. The JM distance for the lodging region and non\_lodging region were employed as an index to examine the annotated quality.

The annotated results were analyzed after fields diving and lodging area annotation (Figure 4). The analysis of the annotated results included three parts as the experiment design in section 2.3.3: algorithm validity verification, feature selection and algorithm generalization performance test.



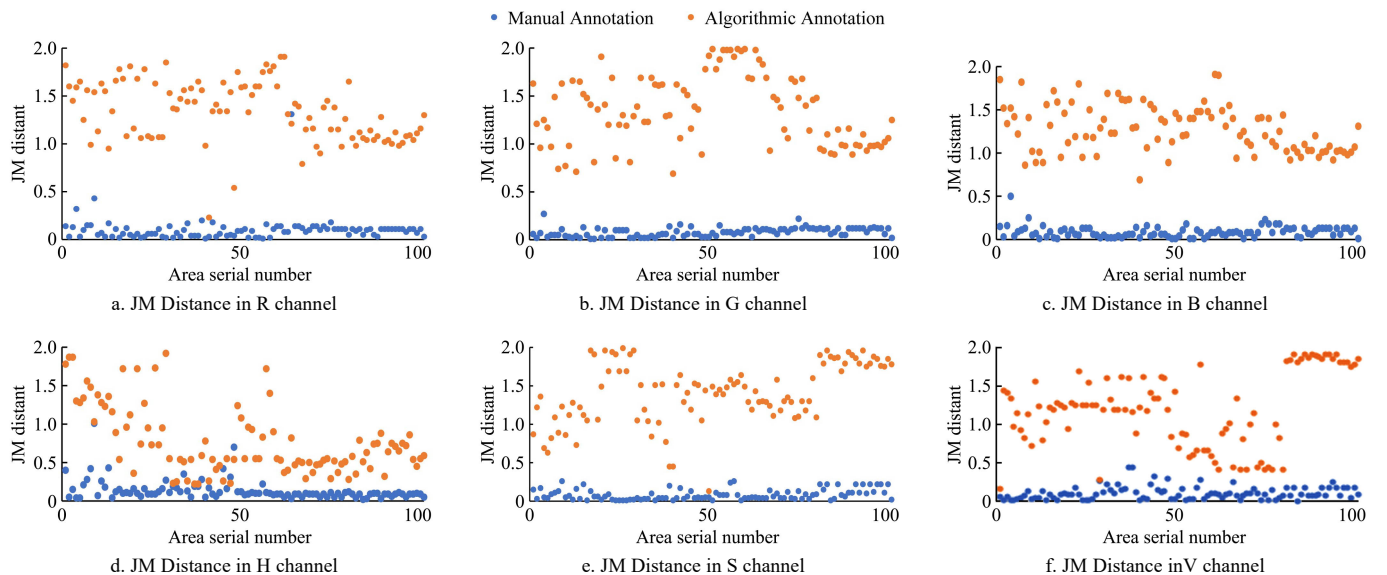
a. Original image

b. Lodging area segmentation

Figure 4 The lodging Area of wheat field

#### 3.1 Algorithm validity verification

The JM distance of the lodging and non\_lodging areas for the manual and algorithm annotation images were compared. The results are presented in Figure 5 and Table 6.



a. JM Distance in R channel

b. JM Distance in G channel

c. JM Distance in B channel

d. JM Distance in H channel

e. JM Distance in S channel

f. JM Distance in V channel

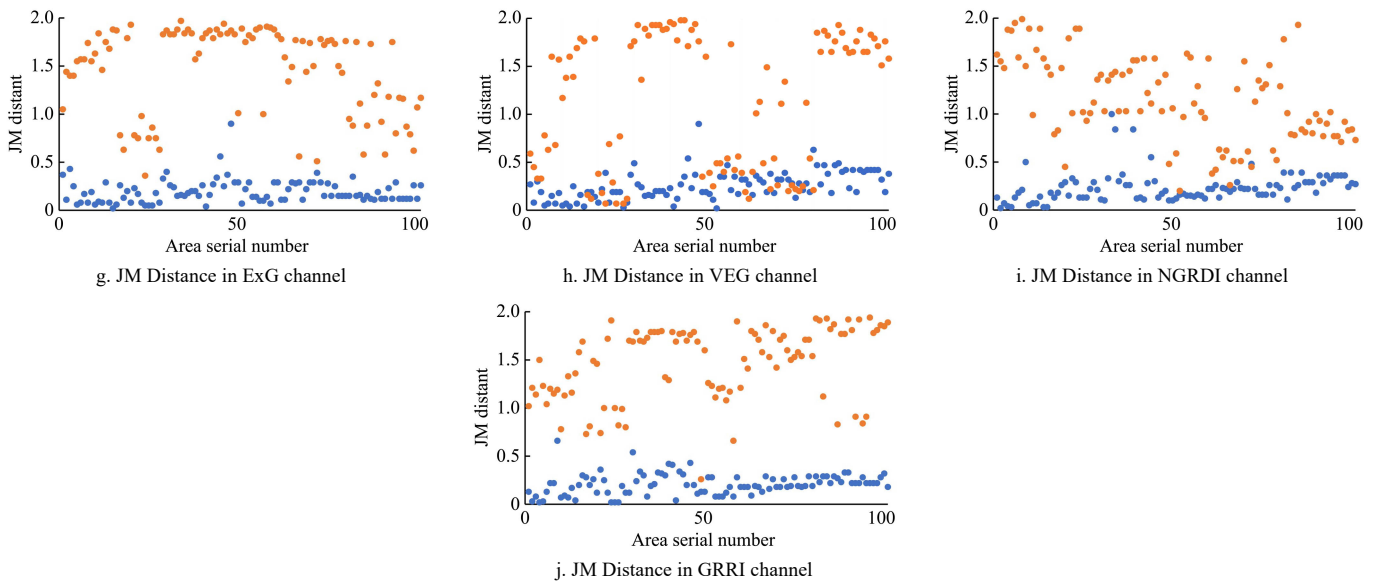


Figure 5 Comparison of the JM distance of the lodging and non\_lodging areas for the manual and algorithm annotation images

**Table 6 Analysis of the JM distance of the lodging and non\_lodging areas for the manual and algorithm annotation images**

Feature		Mean	Variance	Median	Max	Min
R	Algorithm	1.33	0.10	1.34	1.91	0.23
	Manual	0.09	0.01	0.09	0.43	0.01
RGB	G	1.35	0.14	1.36	1.99	0.69
	Manual	0.08	0.01	0.08	0.27	0.01
B	Algorithm	1.28	0.07	1.25	1.91	0.69
	Manual	0.09	0.01	0.08	0.50	0.01
H	Algorithm	0.77	0.19	0.59	1.92	0.22
	Manual	0.14	0.02	0.10	1.01	0.02
HSV	S	1.41	0.16	1.44	1.99	0.13
	Manual	0.09	0.01	0.06	0.26	0.01
V	Algorithm	1.20	0.22	1.23	1.92	0.16
	Manual	0.11	0.01	0.09	0.44	0.01
ExG	Algorithm	1.45	0.20	1.63	1.97	0.36
	Manual	0.19	0.01	0.16	0.90	0.02
VEG	Algorithm	1.14	0.49	1.39	1.98	0.07
	Manual	0.26	0.02	0.23	0.90	0.02
NGRDI	Algorithm	1.15	0.20	1.06	1.99	0.20
	Manual	0.23	0.02	0.22	1.00	0.02
GRRI	Algorithm	1.47	0.14	1.58	1.94	0.26
	Manual	0.21	0.01	0.20	0.66	0.02

As shown in Figure 4, most of the JM distances obtained by the algorithm annotation method was larger than those determined using the manual annotated method. But there were still some points mixed together, it was of great importance to analysis the significance of the differences for JM distances obtained by the algorithm annotation method and the manual annotation method. In the Table 7, the analysis results indicated that the F-value was significantly larger than the F crit value and P-Value values were all close to 0. It was displayed that the results of algorithm and

manual annotation were significantly different. Thus, the annotation method proposed in this study outperforms the manual annotation method.

### 3.2 Feature selection

The JM distance of the lodging and non-lodging regions annotated in 10 features were compared to determine the optimal feature for lodging region annotation. The experimental results are presented in Figure 6 and Table 8.

The experimental results indicated that the JM distance of lodging and non-lodging areas in 10 features were highly variable, especially in GRRI and ExG vegetation index, the median and mean value of JM distance were the largest, the mean and median values of GRRI were 1.47 and 1.58, respectively, and the mean and median values of ExG were 1.45 and 1.63, respectively. The mean and median indexes of the JM distance in GRRI and ExG ranked in the top 2, thus suggesting that the selected feature exhibits high separability. Accordingly, GRRI and ExG were the optimal features for lodging area annotation. The reason for the above experimental results is that the lodging features are most significant in GRRI and ExG.

Furthermore, maximum and minimum indexes of JM distance in GRRI and ExG were analyzed. The maximum values reached 1.94 and 1.97, respectively, and the variance was 0.14. The minimum values were 0.26 and 0.36, respectively, and the variance was 0.20. The above result suggests that there are fewer images with unsatisfactory annotation results, and the algorithm has high adaptability.

In brief, the indexes for image annotated results were ranked (Table 9).

The above experimental results were consistent with the results of existing research<sup>[33,34]</sup>, thus suggesting that ExG and GRRI are the optimal feature for lodging area extraction.

**Table 7 Difference analysis between algorithm and manual annotation results**

Feature	RGB			HSV			ExG	VEG	NGRDI	GRRI
	R	G	B	H	S	V				
F	1288.18	1189.68	1807.97	206.94	1151.38	531.38	780.90	166.92	363.55	1182.20
P-value	0.00	0.00	0.00	0.00	0.00	0.00	0.00	0.00	0.00	0.00
F crit	3.94	3.94	3.94	3.94	3.94	3.94	3.94	3.94	3.94	3.94

Note: P-value values were less than 0.001 and close to 0.

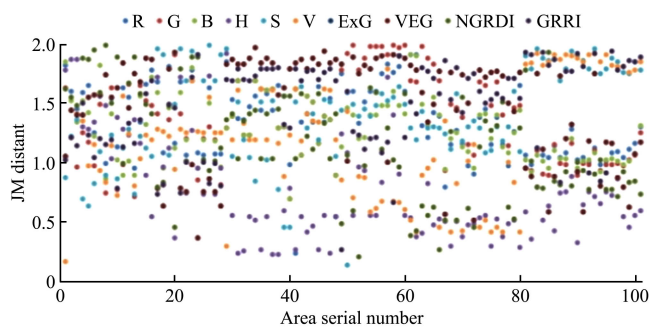


Figure 6 Comparison of the JM distance of the lodging and non\_lodging areas for the manual and algorithm annotation images in 10 features

Table 8 Analysis of the JM distance of the lodging and non\_lodging areas for the manual and algorithm annotation images in 10 features

Feature	Mean	Variance	Median	Max	Min	
RGB	R	1.33	0.10	1.34	1.91	0.23
	G	1.35	0.14	1.36	1.99	0.69
	B	1.28	0.07	1.25	1.91	0.69
HSV	H	0.77	0.19	0.59	1.92	0.22
	S	1.41	0.16	1.44	1.99	0.13
	V	1.20	0.22	1.23	1.92	0.16
ExG	1.45	0.20	1.63	1.97	0.36	
VEG	1.14	0.49	1.39	1.98	0.07	
NGRDI	1.15	0.20	1.06	1.99	0.20	
GRRI	1.47	0.14	1.58	1.94	0.26	

Table 9 Ranking of evaluation indicators for annotation results of wheat field lodging areas under different features

Rank	Mean	Variance	Median	Max	Min
1	GRRI	GRRI	ExG	G	B
2	ExG	ExG	GRRI	S	G
3	S	S	S	NGRDI	ExG
4	G	G	VEG	VEG	GRRI
5	R	R	G	ExG	R
6	B	B	R	GRRI	H
7	V	V	B	H	NGRDI
8	NGRDI	NGRDI	V	V	V
9	VEG	VEG	NGRDI	B	S
10	H	H	H	R	VEG

3.3 Algorithm generalization performance test

In this subsection, the image annotated results at the flowering, filling and mature periods in GRRI and ExG were compared and the generalization performance of the proposed lodging annotation method at different fertility periods were examined. The experimental results are shown in Figure 6 and Table 9.

In flowering period, for images captured in 2019 and 2021, the JM distance of the images in GRRI and ExG were generally good or good and the JM distance for ExG was better than that for GRRI. In the filling period and mature period, for the images captured in 2019 and 2021, the JM distance for GRRI and ExG were the same rating as that in flowering period. In both two years, in the filling period, the JM distance for the images in GRRI was slightly better than that of the images in ExG. Besides, in the mature period, the JM distance for the images in ExG was slight better than that for images in GRRI in 2019, whereas the results were the opposite in 2021. The above experiment results indicated that the JM distance for the images in the two lodging partitioning vegetation index performed differently at different fertility periods and differed from year to year.

The reason for the above discrepant results may be that the light intensity was too high when the images were collected at the filling and mature periods in 2021 and the images were too bright. The image color in ExG was sensitive to strong light and cannot accurately distinguish the characteristics of lodging and non-lodging areas. Thus, it is recommended to select appropriate image acquisition time to stable light intensity when the technology is popularized and used.

Furthermore, the analysis of variance and maximum and minimum indicators (Figure 7, Table 10) indicated that the proportion of poor images in the image annotation results of the three fertility periods was smaller, thus suggesting that the algorithm proposed in this study has excellent generalization performance.

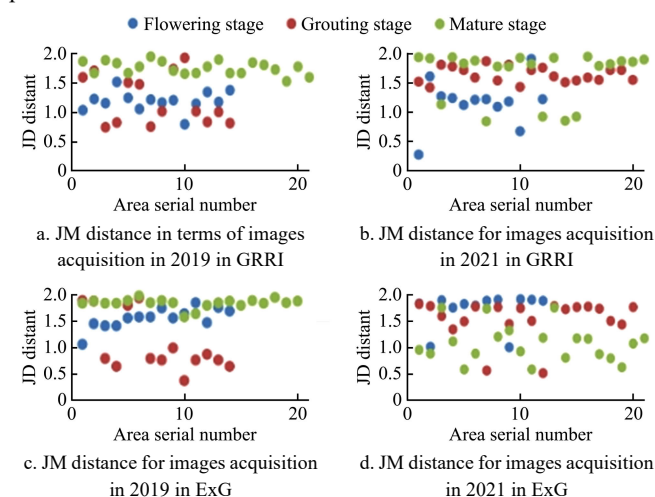


Figure 7 Image annotation results of the images in flowering, filling and mature periods in GRRI and ExG

Table 10 Analysis of image annotation results at the flowering, filling and mature periods in GRRI and ExG

Vegetable Index	Year	Fertility period	Mean	Variance	Median	Max	Min
GRRI	2019	Flowering period	1.17	0.03	1.18	1.50	0.78
		Filling period	1.20	0.18	1.00	1.91	0.73
		Mature period	1.74	0.01	1.76	1.93	1.51
	2021	Flowering period	1.16	0.17	1.21	1.90	0.26
		Filling period	1.63	0.02	1.59	1.86	1.41
		Mature period	1.64	0.17	1.82	1.94	0.83
ExG	2019	Flowering period	1.55	0.04	1.56	1.84	1.05
		Filling period	1.05	0.31	0.78	1.93	0.36
		Mature period	1.83	0.01	1.84	1.97	1.57
	2021	Flowering period	1.71	0.11	1.86	1.91	1.00
		Filling period	1.54	0.14	1.73	1.82	0.51
		Mature period	1.07	0.12	1.07	1.75	0.58

4 Conclusions

A wheat field lodging annotated method based on semi-automatic image segmentation algorithm was proposed to address the low accuracy and subjective problems of the conventional manual annotation method. The proposed method can increase the accuracy of image annotation by extracting lodging areas based on semi-automatic image segmentation algorithm. The conclusion of this study is drawn as follows:

- (1) The image annotation method proposed in this study outperforms the manual image annotation method.
- (2) GRRI and ExG were the most suitable vegetation index for image annotation.

(3) The method in this study exhibits high generalization performance for the images of the three fertility periods, and the percentage of poorer image annotation results is relatively small.

There is still improvement space for the algorithm proposed in this study due to the limitation of experimental conditions. The model does not take into account meteorological factors such as light, temperature and wind speed, and the optimal vegetation index recommended by the model needs to be verified with images of other planting areas. In subsequent research, the effects of external environmental factors (e.g., light, temperature, and wind) on the annotation of wheat field lodging areas will be discussed for the application of the algorithm.

## Funding

This study was financially supported by the Key Research and Technology Development Projects of Anhui Province under Grant 202004a06020045, and the Open Research Fund of National Engineering Research Center for Agro-Ecological Big Data Analysis & Application (grant no. AE202105 and AE202201).

## References

- [1] Liu T X, Guan C Y, Lei D Y. The Research Progress on Evaluation Methods of Lodging Resistance in Crops. *Chinese Agricultural Science Bulletin*, 2007(5): 203–206. doi: none.
- [2] Fan X P, Zhou J P, Xu Y. Research Advances of Monitoring Agricultural Information Using UAV Low-Altitude Remote Sensing. *Journal of Xinjiang University (Natural Science Edition in Chinese and English)*, 2021, 38: 623–31. doi: 10.13568/j.cnki.651094.651316.2020.09.26.0002
- [3] Dong J H, Yang X D, G L, et al. Extraction of winter wheat lodging area information based on UAV remote sensing images. *Heilongjiang Agriculture Sciences*, 2016(10): 147–52. doi: 10.11942/j.issn1002-2767.2016.10.0147
- [4] Yang M D, Huang K S, Kuo Y H, et al. Spatial and Spectral Hybrid Image Classification for Rice Lodging Assessment through UAV Imagery. *Remote Sensing*, 2017, 9(6). doi: 10.3390/rs9060583
- [5] Tian M L, Ban S t, Y T, et al. Monitoring of lodged rice using low-altitude UAV based multispectral image. *Acta Agriculturae Shanghai*, 2018, 34: 88–93. doi: 10.15955/j.issn1000-3924.2018.06.18
- [6] Li G, Zhang L Y, Song C Y, et al. Extraction Method of Wheat Lodging Information Based on Multi-temporal UAV remote sensing data.. *Transactions of the Chinese Society of Agricultural Machinery*, 2019, 50: 211–20. doi: 10.6041/j.issn.1000-1298.2019.04.024
- [7] Ren Z Q, Ding L X, Liu L J, et al. Crop acreage monitoring based on UAV image. *Bulletin of Surveying and Mapping*, 2020, 76–81. doi: 10.13474/j.cnki.11-2246.2020.0218
- [8] Han L, Yang G, Yang X, et al. An explainable XGBoost model improved by SMOTE-ENN technique for maize lodging detection based on multi-source unmanned aerial vehicle images. *Comput Electron Agr*, 2022, 194: 106804. doi: 10.1016/j.compag.2022.106804
- [9] Wang J, Ge H, Dai Q, et al. Unsupervised discrimination between lodged and non-lodged winter wheat: a case study using a low-cost unmanned aerial vehicle. *Int J Remote Sens*, 2018, 39(8): 2079–2088. doi: 10.1080/01431161.2017.1422875
- [10] Li G, Han W, Huang S, et al. Extraction of Sunflower Lodging Information Based on UAV Multi-Spectral Remote Sensing and Deep Learning. *Remote sensing*, 2021, 13(14): 2721. doi: 10.3390/rs13142721
- [11] Tan S, Mortensen A K, Ma X, et al. Assessment of grass lodging using texture and canopy height distribution features derived from UAV visual-band images. *Agr Forest Meteorol*, 2021, 308–309: 108541. doi: 10.1016/j.agrformet.2021.108541. doi: 10.1016/j.imavis.2018.09.017
- [12] Bhagat P K, Choudhary P. Image annotation: Then and now. *Image Vision Comput*, 2018, 80: 1–23. doi: 10.1016/j.imavis.2018.09.017
- [13] D. Bratasanu, I. Nedelcu, M. Datcu, Bridging the semantic gap for satellite image annotation and automatic mapping applications, *IEEE J. Sel. Top. Appl. Earth Obs. Remote. Sens.* 4 (1) (2011) 193–204. doi: none.
- [14] Song L Y, Luo M N, Liu L, et al. Sparse multi-modal topical coding for image annotation. *Neurocomputing*, 214(2016): 162–174. doi: 10.1016/j.neucom.2016.06.005
- [15] Ke X, Li S Z, Cao D L. A two-level model for automatic image annotation. *Multimed Tools Appl*, 2011, 61(1): 195–212. doi: 10.1007/s11042-010-0706-9
- [16] Kong D G, Ding C, Huang H, et al. Multi-label ReliefF and F-statistic featureselections for image annotation, 2012 IEEE Conference on Computer Vision and Pattern Recognition, 2012. pp. 2352–2359. doi: 10.1109/CVPR.2012.6247947
- [17] Jia X, Sun F M, Li H J, et al. Image multi-label annotation based on supervised nonnegative matrix factorization with new matching measurement, *Neurocomputing* 219 (Supplement C) (2017) 518–525. doi: 10.1016/j.neucom.2016.09.052
- [18] Lin Y Q, Lv F J, Zhu S H, et al. Large-scale image classification: fast feature extraction and SVM training, *CVPR* 2011, 2011.pp. 1689–1696. doi: 10.1109/CVPR.2011.5995477
- [19] Yu N, Hua K A, Cheng H. A Multi-Directional Search technique for image annotation propagation. *J Vis Commun Image R*, 2012, 23(1): 237–244. doi: 10.1016/j.jvcir.2011.10.004
- [20] Zhu X F, W Nejd, M Georgescu, An adaptive teleportation random walk model for learning social tag relevance, *Proceedings of the 37th International ACM SIGIR Conference on Research &#38; Development in Information Retrieval, SIGIR '14*, ACM, New York, NY, USA, 2014, pp. 223–232. doi: 10.1145/2600428.2609556
- [21] Lei C Y, Liu D, Li W P, et al. Social diffusion analysis with common-interest model for image annotation. *IEEE Trans. Multimedia* 2016, 18(4): 687–701. doi: 10.1109/TMM.2015.2477277
- [22] Tang J H, Hong R, Qi G J, et al. Image annotation by kNN-sparse graph-based label propagation over noisily tagged web images, 14: 1–14: 15. *ACM Trans. Intell. Syst. Technol*, 2011, 2(2). doi: 10.1145/1899412.1899418
- [23] Xu X, A. Shimada, R.-i. Taniguchi, Image annotation by learning label-specific distance metrics. *Image Analysis and Processing-ICIAP2013*, Springer Berlin Heidelberg, Berlin, Heidelberg, 2013, pp. 101–110. doi: none
- [24] M.M. Kalayeh, H. Idrees, M. Shah, NMF-KNN: Image Annotation Using Weighted Multi-view Non-negative Matrix Factorization, 2014IEEEConferenceonComputer Vision and Pattern Recognition, 2014. pp. 184–191. doi: 10.1109/CVPR.2014.31
- [25] Lin Z J, Ding G G, Hu P P. Image auto-annotation via tag-dependent random search over range-constrained visual neighbours. *Multimedia ToolsAppl*. 2015, 74(11): 4091–4116. doi: 10.1007/s11042-013-1811-3
- [26] Wang L, Zhou T H, Lee Y K, et al. An efficient refinement algorithm for multi-label image annotation with correlation model. *Telecommun Syst*, 2015, 60(2): 285–301. doi: 10.1007/s11235-015-0030-9
- [27] Lin J, Yu T, Wang Z J. Rethinking Crowdsourcing Annotation: Partial Annotation With Salient Labels for Multilabel Aerial Image Classification. *IEEE transactions on geoscience and remote sensing*, 2022, 60: 1. doi: 10.1109/TGRS.2022.3191735
- [28] Theodosiou Z, Tsapatsoulis N. Image annotation: the effects of content, lexicon and annotation method. *International Journal of Multimedia Information Retrieval*, 2020, 9(3): 191–203. doi: 10.1007/s13735-020-00193-z
- [29] Ke X, Li S, Cao D. A two-level model for automatic image annotation. *Multimedia Tools and Applications*, 2012, 61(1): 195–212. doi: 10.1007/s11042-010-0706-9
- [30] Wang Y J, Qi Q, Liu Y, et al. Unsupervised segmentation evaluation using area-weighted variance and Jeffries-Matusita distance for remote sensing images. *Remote Sensing*, 2018, 10: 1193. doi: 10.3390/rs10081193
- [31] Qiu B W, Fan Z L, Zhong M, et al. A new approach for crop identification with wavelet variance and JM distance. *Environmental Monitoring and Assessment*, 2014, 186(11): 7929–7940. doi: 10.1007/s10661-014-3977-1
- [32] Liu H L, Zhang F Z, Zhang L F, et al. UNVI-Based Time Series for Vegetation Discrimination Using Separability Analysis and Random Forest Classification. *Remote Sensing*, 2020, 12(3): 529. doi: 10.3390/rs12030529
- [33] Du M, Noguchi N. Monitoring of Wheat Growth Status and Mapping of Wheat Yield's within-Field Spatial Variations Using Color Images Acquired from UAV-camera System. *Remote sensing (Basel, Switzerland)*, 2017, 9(3): 289. doi: 10.3390/rs9030289
- [34] Yang B H, Zhu Y, Zhou S J. Accurate Wheat Lodging Extraction from Multi-Channel UAV Images Using a Lightweight Network Model. *Sensors (Basel, Switzerland)*, 2021, 21(20): 6826. doi: 10.3390/s21206826